

Deuteron-like states composed of two doubly charmed baryons

Lu Meng,^{1,*} Ning Li,^{2,†} and Shi-Lin Zhu^{1,3,‡}

¹*Department of Physics and State Key Laboratory of Nuclear Physics and Technology, Peking University, Beijing 100871, China*

²*Institute for Advanced Simulation, Institut für Kernphysik,*

and Jülich Center for Hadron Physics, Forschungszentrum Jülich, D-52425 Jülich, Germany

³*Collaborative Innovation Center of Quantum Matter, Beijing 100871, China*

We present a systematic investigation of the possible molecular states composed of a pair of doubly charmed baryons ($\Xi_{cc}\Xi_{cc}$) or one doubly charmed baryon and one doubly charmed antibaryon ($\Xi_{cc}\bar{\Xi}_{cc}$) within the framework of the one-boson-exchange-potential model. For the spin-triplet systems, we take into account the mixing between the 3S_1 and 3D_1 channels. For the baryon-baryon system $\Xi_{cc}\Xi_{cc}$ with $(R, I) = (\bar{3}, 1/2)$ and $(\bar{3}, 0)$, where R and I represent the group representation and the isospin of the system, respectively, there exist loosely bound molecular states. For the baryon-antibaryon system $\Xi_{cc}\bar{\Xi}_{cc}$ with $(R, I) = (8, 1), (8, 1/2)$ and $(8, 0)$, there also exist deuteron-like molecules. The $B_{cc}\bar{B}_{cc}$ molecular states may be produced at LHC. The proximity of their masses to the threshold of two doubly charmed baryons provides a clean clue to identify them.

PACS numbers: 12.39.Pn, 14.20.-c, 12.40.Yx

Keywords:

I. INTRODUCTION

In 2003, the Belle Collaboration discovered the charmonium-like state $X(3872)$ [1]. Subsequently, more charmonium-/bottomonium-like states such as $Y(4260)$ [2], $Z_c(3900)$ [3, 4], $Y(4140)$ [5] and $Y_b(10888)$ [6] were observed by the BARBAR, BESIII, Belle, CDF and Belle collaborations respectively. Recently, two hidden-charm pentaquark states $P_c(4380)$ and $P_c(4450)$ were observed by the LHCb Collaboration [7]. The experimental and theoretical progress on the hidden-charm multiquark states can be found in the recent review [8].

It's difficult to accommodate all these XYZ states in the conventional hadron spectrum. Especially the charged charmonium-like states are probably good candidates of multiquark states. Some XYZ states lie very close to the threshold of two charmed hadrons. They are speculated to be candidates of the hadronic molecular states.

A hadronic molecule is a loosely bound state formed by two color-singlet hadrons. The molecular states are bound by the residual strong interaction. For example, the deuteron is a well-established hadronic molecule, which is a loosely bound state formed by the proton and neutron. Its binding energy is about 2.225 MeV and root-mean-square radius around 2.0 fm. Compared to the size of the conventional meson and baryon, the deuteron is really loosely bound. Besides the deuteron, Voloshin and Okun investigated the possible molecular states formed by a charmed meson and a charmed antimeson forty years ago [9]. Also, De Rujula *et al* tried to explain $\psi(4040)$ as a $D^*\bar{D}^*$ molecular state in [10]. In [11, 12], Törnqvist analysed the possible deuteron-like $D\bar{D}^*$ and $D^*\bar{D}$ molecules. In literature, there are many investigations on the hadronic molecules such as the $\Lambda(1405)$ as a candidate of the $\bar{K}N$ molecule [13, 14], the dibaryon composed of two light baryons [15–22], the possible molecular states composed of a pair of heavy mesons [23–29], the molecular states composed of a pair of heavy baryons [30–35], $\Lambda_c\Lambda_c$ and $\Lambda_c N$ bound states [36, 37] and the possible bound states of $\Sigma_c N, \Xi'_c N, \Xi_{cc} N, \Xi\Xi_{cc}$, [38, 39].

Very recently, many events with four heavy quarks ($QQ\bar{Q}\bar{Q}$) were reported by different collaborations. For example, the J/ψ pairs were observed by LHCb [40] and CMS collaborations[41]. The simultaneous $J/\psi\Upsilon(1S)$ events were reported by both D0[42] and CMS[43]. CMS Collaboration also observed the simultaneous $\Upsilon(1S)\Upsilon(1S)$ events[44]. Some of these $QQ\bar{Q}\bar{Q}$ events may be resonant. There are extensive theoretical discussions about the possible $QQ\bar{Q}\bar{Q}$ states [45–50].

In this work, we investigate the possible deuteron-like hadronic molecules composed of two doubly charmed baryons. These states have the configurations such as $\Xi_{cc}\Xi_{cc}$ or $\Xi_{cc}\bar{\Xi}_{cc}$. Especially, the possible $\Xi_{cc}\bar{\Xi}_{cc}$ molecular states can be searched for at LHC. We will adopt the one-boson-exchange-potential model (OBEP). Aside from the long-range

*Electronic address: lmeng@pku.edu.cn

†Electronic address: n.li@fz-juelich.de

‡Electronic address: zhushi@pku.edu.cn

π exchange force [51], the OBEP model also introduces the medium-range σ exchange as well as the short-range ρ and ω exchange forces.

We organize the paper as follows. After the introduction, we present the theoretical formalism including the Lagrangians, the derivations of the coupling constants and the interaction potential in Section II. Our numerical results are given in Section III. We summarize our results and make some discussions in Section IV. Some useful formulae are collected in the Appendix.

II. FORMALISM

In 2002, the SELEX Collaboration reported a doubly charmed state with mass 3520 MeV [52]. This structure contains two charm quarks and a down quark, and it is denoted by Ξ_{cc} . Later this state was confirmed by the same collaboration [53]. In a conference report [54], another state containing two charm quarks and an up quark at 3780 MeV was reported also by the SELEX Collaboration. In Refs. [55–60], the mass of the doubly charmed baryon was estimated from 3511 to 3685 MeV. The particular isospin splitting of the states observed by SELEX was discussed in Ref. [61].

The doubly charmed baryon Ξ_{cc} is composed of two charm quarks and one light quark. The wave function of the two charm quarks is

$$\psi_{cc} = \psi_{cc}^{flavor} \otimes \psi_{cc}^{color} \otimes \psi_{cc}^{spin} \otimes \psi_{cc}^{space}. \quad (1)$$

For the ground state, both the flavor wave function ψ_{cc}^{flavor} and space wave function ψ_{cc}^{space} are symmetric while its color wave function ψ_{cc}^{color} is antisymmetric under the exchange of the two charm quarks. Hence, the spin wave function ψ_{cc}^{spin} is symmetric as required by Pauli Principle, ie., $S_{cc} = 1$. As a result, the spin of Ξ_{cc} for the ground state is $\frac{1}{2}$ or $\frac{3}{2}$. In the present work, we focus on the molecular systems composed of two spin- $\frac{1}{2}$ Ξ_{cc} . They should be the lightest states among molecular states with various spin configurations.

The heavy charm quarks act as the static color source. The doubly charmed baryons form the fundamental representation in the SU(3) flavor space regarding to the light quarks. For convenience, we adopt the notation, $B_{cc} = (\Xi_{cc}^u, \Xi_{cc}^d, \Xi_{cc}^s)^T$, where the superscripts of Ξ_{cc} denote the corresponding light quarks and superscript T means transpose of the matrix.

Under the SU(3)-flavor symmetry, the $B_{cc}B_{cc}$ systems are decomposed as $3_F \otimes 3_F = 6_F \oplus \bar{3}_F$ while the $B_{cc}\bar{B}_{cc}$ systems can be decomposed as $3_F \otimes \bar{3}_F = 8_F \oplus 1_F$. For simplicity, we use (R, I) to denote the systems, where R and I represent the group representation and isospin, respectively. The relevant flavor wave functions are given in Table I.

TABLE I: Flavor wave functions of the $B_{cc}B_{cc}$ and $B_{cc}\bar{B}_{cc}$ systems. R and I denotes the group representation and the isospin respectively.

Systems/ (R, I)	Flavor	Systems/ (R, I)	Flavor	Systems/ (R, I)	Flavor
$(6, 1)$	uu	$(\bar{3}, \frac{1}{2})$	$\frac{1}{\sqrt{2}}(us - su)$	$(8, \frac{1}{2})$	$u\bar{s}$
	$\frac{1}{\sqrt{2}}(ud + du)$		$\frac{1}{\sqrt{2}}(ds - sd)$		$d\bar{s}$
	dd	$(\bar{3}, 0)$	$\frac{1}{\sqrt{2}}(ud - du)$	$(8, \frac{1}{2})$	$s\bar{d}$
$(6, \frac{1}{2})$	$\frac{1}{\sqrt{2}}(us + su)$	$(8, 1)$	$u\bar{d}$	$(8, 0)$	$s\bar{u}$
	$\frac{1}{\sqrt{2}}(ds + sd)$		$\frac{1}{\sqrt{2}}(u\bar{u} - d\bar{d})$		$\frac{1}{\sqrt{6}}(u\bar{u} + d\bar{d} - 2s\bar{s})$
$(6, 0)$	ss		$d\bar{u}$	$(1, 0)$	$\frac{1}{\sqrt{3}}(u\bar{u} + d\bar{d} + s\bar{s})$

TABLE II: The Coupling constants and the masses of the relevant hadrons [62–65]. For the pion and kaon multiplets, their averaged masses are used. $m_{\Xi_{cc}^+}$ is the mass of Ξ_{cc}^+ reported in Ref. [52, 53].

Baryons	Mass (MeV)	Mesons	Mass (MeV)	Mesons	Mass (MeV)	Coupling	Value	Coupling	Value
$\Xi_{cc}^{u,d,s}$	3520	π	137.27	ϕ	1019.46	$g_{\pi NN}^2/4\pi$	13.6	$g_{p hh}$	-13.86
Proton (p)	938.27	η	547.85	K	495.65	$g_{\rho NN}^2/4\pi$	0.84	$g_{v hh}$	4.60
Neutron (n)	939.57	ρ	775.49	K^*	893.80	$f_{\rho NN}/g_{\rho NN}$	6.1	$f_{v hh}$	-29.06
		ω	782.65	σ	600	$g_{\sigma NN}^2/4\pi$	5.69	$g_{\sigma hh}$	2.82

A. The Lagrangian

The notations for the exchanged pseudoscalar and vector mesons read

$$\mathcal{M} = \begin{pmatrix} \frac{\pi^0}{\sqrt{2}} + \frac{\eta}{\sqrt{6}} & \pi^+ & K^+ \\ \pi^- & -\frac{\pi^0}{\sqrt{2}} + \frac{\eta}{\sqrt{6}} & K^0 \\ K^- & \bar{K}^0 & -\frac{2}{\sqrt{6}}\eta \end{pmatrix}, \quad \mathcal{V}^\mu = \begin{pmatrix} \frac{\rho^0}{\sqrt{2}} + \frac{\omega}{\sqrt{2}} & \rho^+ & K^{*+} \\ \rho^- & -\frac{\rho^0}{\sqrt{2}} + \frac{\omega}{\sqrt{2}} & K^{*0} \\ K^{*-} & \bar{K}^{*0} & \phi \end{pmatrix}^\mu. \quad (2)$$

Some heavier-meson exchanges which provide very short-range interactions are not included since we focus on the very loosely bound states. Under the SU(3)-flavor symmetry, we construct the Lagrangian for the pseudoscalar exchange as

$$\mathcal{L}_{p hh} = g_{p hh} \bar{B}_{cc} i \gamma_5 \mathcal{M} B_{cc}. \quad (3)$$

One may also use the axial-vector coupling,

$$\mathcal{L}_{p hh} = f_{p hh} \bar{B}_{cc} \gamma_5 \gamma_\mu \partial^\mu \mathcal{M} B_{cc}, \quad (4)$$

The above two Lagrangians are equivalent at the tree level. In the current calculation, we adopt Eq. (3). For the vector-meson exchange, we have

$$\mathcal{L}_{v hh} = g_{v hh} \bar{B}_{cc} \gamma_\mu \mathcal{V}^\mu B_{cc} + \frac{f_{v hh}}{2m} \bar{B}_{cc} \sigma_{\mu\nu} \partial^\mu \mathcal{V}^\nu B_{cc}, \quad (5)$$

and for the scalar-meson exchange,

$$\mathcal{L}_{\sigma hh} = g_{\sigma hh} \bar{B}_{cc} \sigma B_{cc}. \quad (6)$$

In the previous expressions, $g_{p hh}$, $g_{v hh}$, $f_{v hh}$ and $g_{\sigma hh}$ are the coupling constants. Their values are given in Section II B.

B. Coupling Constants

In this subsection, we focus on the derivation of the coupling constants used in the current work. The coupling constants for the light bosons interacting with the nucleon are relatively well-known. They can either be extracted from experimental data or calculated from various models. We will derive the values of the coupling constants with the help of the quark model. We denote the coupling constants between the light mesons and the doubly charmed baryons as $g_{m B_{cc} B_{cc}}$, those between the light mesons and the quarks as $g_{m qq}$, and those between the light mesons and the nucleon as $g_{m NN}$. We make use of the relations as follows,

$$\langle p \uparrow | \mathcal{L}_{m NN} | p \uparrow \rangle = \langle p \uparrow | \mathcal{L}_{m qq} | p \uparrow \rangle, \quad (7)$$

$$\langle \Xi_{cc}^u \uparrow | \mathcal{L}_{m hh} | \Xi_{cc}^u \uparrow \rangle = \langle \Xi_{cc}^u \uparrow | \mathcal{L}_{m qq} | \Xi_{cc}^u \uparrow \rangle. \quad (8)$$

where “ \uparrow ” means the third component of the spin is $+1/2$. The matrix elements are calculated both at hadron and quark level respectively. We first derive the relation between $g_{m qq}$ and $g_{m NN}$ from Eq. (7), and then obtain the

relation between $g_{mB_{cc}B_{cc}}$ and g_{mqq} from Eq. (8). Both relations contain quark masses. Finally, we combine the two relations and obtain the relation between $g_{mB_{cc}B_{cc}}$ and g_{mNN} without the quark mass dependence.

At the hadron level, the Lagrangians for the light mesons and the nucleon are

$$\mathcal{L}_{\pi NN} = g_{\pi NN} \bar{N} i \gamma_5 \boldsymbol{\tau} \cdot \boldsymbol{\pi} N, \quad (9)$$

$$\mathcal{L}_{\rho NN} = g_{\rho NN} \bar{N} \boldsymbol{\gamma}_\mu \boldsymbol{\tau} \cdot \boldsymbol{\rho}^\mu N + \frac{f_{\rho NN}}{2m_N} \bar{N} \boldsymbol{\sigma}_{\mu\nu} (\boldsymbol{\tau} \cdot \partial^\mu \boldsymbol{\rho}^\nu) N, \quad (10)$$

$$\mathcal{L}_{\sigma NN} = g_{\sigma NN} \bar{N} \sigma N, \quad (11)$$

where $N = (p, n)^T$ with p and n the proton and neutron respectively. The numerical values of the coupling constants, $g_{\pi NN}$, $g_{\rho NN}$, $f_{\rho NN}$ and $g_{\sigma NN}$ are taken from Refs. [62–64] and collected in Table II.

At the quark level, the Lagrangian reads

$$\mathcal{L}_q = g_{pqq} \bar{q} i \gamma_5 \mathcal{M} q + g_{vqq} \bar{q} \boldsymbol{\gamma}_\mu \mathcal{V}^\mu q + g_{\sigma qq} \bar{q} \sigma q \quad (12)$$

where $q = (u, d, s)^T$ is the light quark triplet. Notice that in the above expression we do not consider the tensor part as we do at the hadron level (the second part of the Eq. (10)) for the vector-meson exchange because the quarks are taken as point particles whereas the hadrons are not.

The amplitudes for the two baryons and π^0 vertices read,

$$i\mathcal{M}_{\pi^0 p \uparrow p \uparrow} = g_{\pi NN} \frac{Q_3}{m_N} = \frac{1}{\sqrt{2}} g_{pqq} \frac{Q_3}{m_q} \times \frac{5}{3}, \quad (13)$$

$$i\mathcal{M}_{\pi^0 \Xi_{cc}^u \uparrow \Xi_{cc}^u \uparrow} = \frac{1}{\sqrt{2}} g_{pqq} \frac{Q_3}{m_{\Xi_{cc}}} = \frac{1}{\sqrt{2}} g_{pqq} \frac{Q_3}{m_q} \times \left(-\frac{1}{3}\right), \quad (14)$$

where m_q , m_N and $m_{\Xi_{cc}}$ are the masses of the quark, nucleon and doubly charmed baryon respectively while Q_3 is the third component of the pion momentum. With the above relation, one obtain g_{pqq} directly. Finally, we obtain the all coupling constants used in the current work as

$$g_{\sigma hh} = \frac{1}{3} g_{\sigma NN}, \quad g_{p hh} = -\frac{\sqrt{2}}{5} \frac{m_{\Xi_{cc}}}{m_N} g_{\pi NN}, \quad (15)$$

$$g_{v hh} = \sqrt{2} g_{\rho NN}, \quad g_{v hh} + f_{v hh} = -\frac{\sqrt{2}}{5} (g_{\rho NN} + f_{\rho NN}) \frac{m_{\Xi_{cc}}}{m_N}, \quad (16)$$

For the vector-meson exchange, we use the values of $g_{\rho NN}$ but not $g_{\omega NN}$ because $g_{\rho NN}$ is more stable than $g_{\omega NN}$ in different models. The numerical values of the coupling constants are given in Table II. For the doubly charmed baryon masses, we assume the exact SU(3)-flavor symmetry and take the results from the SELEX Collaboration [52], 3520 MeV, for all the doubly charmed baryons covered in the work.

C. The Interaction Potentials

With the Lagrangians in Section II A, we derive the interaction potentials in momentum space. Due to the large masses of the doubly charmed baryons, the interaction potential in the momentum space $V(\mathbf{Q})$ is expanded in terms of $\mathbf{Q}/m_{\Xi_{cc}}$, or $\mathbf{k}/m_{\Xi_{cc}}$, where \mathbf{Q} is $(\mathbf{p}_f - \mathbf{p}_i)$ while \mathbf{k} is $(\mathbf{p}_i + \mathbf{p}_j)/2$, and kept up to order $\mathcal{O}(\mathbf{Q}^2/m_{\Xi_{cc}}^2, \mathbf{k}^2/m_{\Xi_{cc}}^2)$. In our case, Q_0^2 is in fact a high order term and can be neglected directly, see Appendix A for a short analysis of Q_0^2 . After transforming the potential into the coordinate space, the conjugate variable of \mathbf{Q} is \mathbf{r} and that of \mathbf{k} is $-i\nabla$. The latter provides the only nonlocal potential in the present calculations, i.e. the spin-orbit force. Other nonlocal interactions such as the recoil effect are neglected. It is mentioned in Ref. [62] that the nonlocal potential changes the off-shell behavior. However, in the present work we are mainly interested in the hadronic molecular states composed of the doubly charmed baryons, in which the bounded hadrons are approximately on-shell. Hence, it is reasonable to neglect the nonlocal potential other than the spin-orbit force in our calculation.

When performing the Fourier Transformation, we introduce a monopole form factor,

$$\mathcal{F}(\mathbf{Q}) = \frac{\Lambda^2 - m_{ex}^2}{\Lambda^2 - Q^2} = \frac{\Lambda^2 - m_{ex}^2}{\lambda^2 + Q^2}, \quad (17)$$

for each vertex. Λ is a cutoff parameter, which is used to suppress the high-momenta contribution or equivalently, to soften the short-range interactions. m_{ex} and Q are the mass and four momentum of the exchanged meson respectively,

and $\lambda^2 = \Lambda^2 - Q_0^2$. After the Fourier Transformation,

$$\mathcal{V}(r) = \frac{1}{(2\pi)^3} \int d\mathbf{Q} e^{i\mathbf{Q}\cdot\mathbf{r}} \mathcal{V}(\mathbf{Q}) \mathcal{F}^2(\mathbf{Q}), \quad (18)$$

one obtains the interaction potentials in coordinate space which read

- Pseudoscalar exchange:

$$\begin{aligned} \mathcal{V}_{SS}^p(r; \alpha) &= C_\alpha^p \frac{g_{1p}g_{2p}}{4\pi} \frac{m_\alpha^3}{12m_{\Xi cc}^2} H_1(\Lambda, m_\alpha, r) \boldsymbol{\sigma}_1 \cdot \boldsymbol{\sigma}_2, \\ \mathcal{V}_T^p(r; \alpha) &= C_\alpha^p \frac{g_{1p}g_{2p}}{4\pi} \frac{m_\alpha^3}{12m_{\Xi cc}^2} H_3(\Lambda, m_\alpha, r) S_{12}(\hat{r}), \end{aligned} \quad (19)$$

- Vector exchange:

$$\begin{aligned} \mathcal{V}_C^v(r; \beta) &= C_\beta^v \frac{m_\beta}{4\pi} \left[g_{1v}g_{2v}H_0(\Lambda, m_\beta, r) + \frac{m_\beta^2}{8m_{\Xi cc}^2} (g_{1v}g_{2v} + 2g_{1v}f_{2v} + 2g_{2v}f_{1v})H_1(\Lambda, m_\beta, r) \right], \\ \mathcal{V}_{SS}^v(r; \beta) &= C_\beta^v [g_{1v}g_{2v} + g_{1v}f_{2v} + g_{2v}f_{1v} + f_{1v}f_{2v}] \frac{1}{4\pi} \frac{m_\beta^3}{6m_{\Xi cc}^2} H_1(\Lambda, m_\beta, r) \boldsymbol{\sigma}_1 \cdot \boldsymbol{\sigma}_1, \\ \mathcal{V}_T^v(r; \beta) &= -C_\beta^v [g_{1v}g_{2v} + g_{1v}f_{2v} + g_{2v}f_{1v} + f_{1v}f_{2v}] \frac{1}{4\pi} \frac{m_\beta^3}{12m_{\Xi cc}^2} H_3(\Lambda, m_\beta, r) S_{12}(\hat{r}), \\ \mathcal{V}_{LS}^v(r; \beta) &= -C_\beta^v \frac{1}{4\pi} \frac{m_\beta^3}{2m_{\Xi cc}^2} H_2(\Lambda, m_\beta, r) [3g_{1v}g_{2v} \mathbf{L} \cdot \mathbf{S} + 4g_{2v}f_{1v} \mathbf{L} \cdot \mathbf{S}_1 + 4g_{1v}f_{2v} \mathbf{L} \cdot \mathbf{S}_2], \end{aligned} \quad (20)$$

- Scalar exchange:

$$\begin{aligned} \mathcal{V}_C^s(r; \sigma) &= -C_\sigma^s m_\sigma \frac{g_{1s}g_{2s}}{4\pi} \left[H_0(\Lambda, m_\sigma, r) - \frac{m_\sigma^2}{8m_{\Xi cc}^2} H_1(\Lambda, m_\sigma, r) \right], \\ \mathcal{V}_{LS}^s(r; \sigma) &= -C_\sigma^s \frac{g_{1s}g_{2s}}{4\pi} \frac{m_\sigma^3}{2m_{\Xi cc}^2} H_2(\Lambda, m_\sigma, r) \mathbf{L} \cdot \mathbf{S}. \end{aligned} \quad (21)$$

In the above expressions, the superscripts p , s and v denote the pseudoscalar, scalar and vector mesons, respectively. $\alpha = \pi, \eta$ or K while $\beta = \omega, \rho, \phi$ and K^* . The specific expressions of the scalar functions H_0, H_1, H_2 and H_3 are given in Appendix A. Some details about the so-called "contact interaction" are also included in Appendix A. C_α^p, C_β^v and C_σ^s are the isospin factors. Their numerical values are given in Table III. \mathbf{L} is the relative orbit angular momentum operator between the two baryons while $\mathbf{S}_{1(2)}$ is the spin operator for baryon 1(2). The total spin operator of the two-baryon system is $\mathbf{S} = \mathbf{S}_1 + \mathbf{S}_2$. $S_{12}(\hat{r}) = 3(\boldsymbol{\sigma}_1 \cdot \hat{r})(\boldsymbol{\sigma}_2 \cdot \hat{r}) - \boldsymbol{\sigma}_1 \cdot \boldsymbol{\sigma}_2$ is the tensor operator which mixes the S - and D -waves.

With the specific expressions in Eqs. (19-21) and the isospin factors given in Table III, one can obtain the potentials for the $B_{cc}B_{cc}$ systems. Instead of calculating Feynman amplitude of tree diagram, we can use the "G-parity" rule to derive the potentials of the $B_{cc}\bar{B}_{cc}$ systems directly from the potentials for the $B_{cc}B_{cc}$ systems if the exchanged meson has certain "G-parity". For example, one immediately obtains the pion-exchange potential for the $B_{cc}\bar{B}_{cc}$ system with $(R, I) = (8, 1)$ by multiplying the corresponding potential for the $B_{cc}B_{cc}$ system with $(R, I) = (6, 1)$ by an factor $(-1)^{G_\pi}$ where G_π is the "G-parity" of the pion, see Table III. For the baryon-antibaryon systems, some annihilation potentials corresponding to the very short-range interactions are not included in the current calculation since we focus on the study of the loosely bound states.

Since we focus on the system composed of a pair of spin- $\frac{1}{2}$ particles, the total spin of the system can be 0 or 1. For the spin-0 case, we focus on the 1S_0 channel while for the spin-1 case we must deal with the 3S_1 and 3D_1 simultaneously because of the tensor potential. The wave functions of the spin-singlet channel read

$$\Psi(r, \theta, \phi) \chi_{ss_z} = y_S(r) |^1S_0\rangle, \quad (22)$$

while the wave functions of the spin-triplet channels are

$$\Psi(r, \theta, \phi)^T \chi_{ss_z}^T = \begin{pmatrix} T_S(r) \\ 0 \end{pmatrix} |^3S_1\rangle + \begin{pmatrix} 0 \\ T_D(r) \end{pmatrix} |^3D_1\rangle, \quad (23)$$

TABLE III: The isospin factors. R and I denote the group representation and isospin respectively. The left panel is for the $B_{cc}B_{cc}$ system while the right panel is for the $B_{cc}\bar{B}_{cc}$ system.

Systems/ (R, I)	C_π^p	C_η^p	C_K^p	C_ρ^v	C_ω^v	C_ϕ^v	$C_{K^*}^v$	C_σ^s	Systems/ (R, I)	C_π^p	C_η^p	C_K^p	C_ρ^v	C_ω^v	C_ϕ^v	$C_{K^*}^v$	C_σ^s
(6, 1)	$\frac{1}{2}$	$\frac{1}{6}$	0	$\frac{1}{2}$	$\frac{1}{2}$	0	0	1	(8, 1)	$-\frac{1}{2}$	$\frac{1}{6}$	0	$\frac{1}{2}$	$-\frac{1}{2}$	0	0	1
(6, $\frac{1}{2}$)	0	$-\frac{1}{3}$	1	0	0	0	1	1	(8, $\frac{1}{2}$)	0	$-\frac{1}{3}$	0	0	0	0	0	1
(6, 0)	0	$\frac{2}{3}$	0	0	0	1	0	1	(8, $\frac{1}{2}$)	0	$-\frac{1}{3}$	0	0	0	0	0	1
($\bar{3}$, $\frac{1}{2}$)	0	$-\frac{1}{3}$	-1	0	0	0	-1	1	(8, 0)	$\frac{1}{2}$	$\frac{1}{2}$	$-\frac{4}{3}$	$-\frac{1}{2}$	$-\frac{1}{6}$	$-\frac{2}{3}$	$\frac{4}{3}$	1
($\bar{3}$, 0)	$-\frac{3}{2}$	$\frac{1}{6}$	0	$-\frac{3}{2}$	$\frac{1}{2}$	0	0	1	(1, 0)	1	$\frac{1}{3}$	$\frac{4}{3}$	-1	$-\frac{1}{3}$	$-\frac{1}{3}$	$-\frac{4}{3}$	1

In Eq. (22), $y_S(r)$ is the radial wave function for the 1S_0 channel while $T_S^T(r)$ and T_D^T in Eq. (23) are the radial wave functions for 3S_1 and 3D_1 channels, respectively. For the matrices of the operators appearing in Eqs. (19-21), we have

- Spin-singlet ($S = 0$):

$$\boldsymbol{\sigma}_1 \cdot \boldsymbol{\sigma}_2 = -3, \quad \mathbf{L} \cdot \mathbf{S} = 0, \quad \mathbf{L} \cdot \mathbf{S}_1 = 0, \quad \mathbf{L} \cdot \mathbf{S}_2 = 0, \quad S_{12}(\hat{r}) = 0, \quad (24)$$

- Spin-triplet ($S = 1$):

$$\boldsymbol{\sigma}_1 \cdot \boldsymbol{\sigma}_2 = \begin{pmatrix} 1 & 0 \\ 0 & 1 \end{pmatrix}, \quad S_{12}(\hat{r}) = \begin{pmatrix} 0 & \sqrt{8} \\ \sqrt{8} & -2 \end{pmatrix}, \quad \mathbf{L} \cdot \mathbf{S} = \begin{pmatrix} 0 & 0 \\ 0 & -3 \end{pmatrix}, \quad (25)$$

$$\mathbf{L} \cdot \mathbf{S}_1 = \begin{pmatrix} 0 & 0 \\ 0 & -\frac{3}{2} \end{pmatrix}, \quad \mathbf{L} \cdot \mathbf{S}_2 = \begin{pmatrix} 0 & 0 \\ 0 & -\frac{3}{2} \end{pmatrix}. \quad (26)$$

One may find the details in deriving these matrices in Appendix B.

III. NUMERICAL RESULTS

We solve the Schrödinger equation with the potential derived before and obtain the binding energy (B. E.) and the radial wave function. With the wave functions we also calculate the root-mean-square radius r_{rms} . The root-mean-square radius reads

$$r_{rms}^2 = \int y_S^*(r)y_S(r)r^4 dr, \quad (27)$$

for the spin-singlet channels and

$$r_{rms}^2 = \int [T_S^*(r)T_S(r) + T_D^*(r)T_D(r)]r^4 dr, \quad (28)$$

for the spin-triplet channels. For the coupled channels, we also calculate the individual probability for each channel,

$$P_{3S_1} = \int T_S^*(r)T_S(r)r^2 dr, \quad (29)$$

for the 3S_1 channel and

$$P_{3D_1} = \int T_D^*(r)T_D(r)r^2 dr, \quad (30)$$

for the 3D_1 channel.

In our calculation, we need the value of the cutoff. The study of the deuteron with the OBEP model suggests a reasonable range for the cutoff, 0.80 – 1.50 GeV. Since the doubly charmed baryon is much heavier than the nucleon, we take a slightly wider range 0.8 – 2.0 GeV for the cutoff parameter.

A. $B_{cc}B_{cc}$ systems

For the $B_{cc}B_{cc}$ systems, the total wave functions should be antisymmetric under exchange of the two baryons, required by Pauli Principle. Given that the spacial wave functions are symmetric (S or D waves), the spin of the system is 1 and 0 for the $\bar{3}$ -representation and 6-representation respectively.

1. $\bar{3}$ -representation, $S = 1$

Since the spins of the systems belonging to the $\bar{3}$ -representation are 1, the 3S_1 and 3D_1 channels couple with each other. We plot the potentials for each exchanged boson in Fig. 1. From the plots, one can see clearly that for the $(R, I) = (\bar{3}, 0)$ case, the π - and ω -exchanges provide repulsive potential while the ρ - and σ -exchanges supply the attractive force in the 3S_1 channel. The contribution of the η -exchange is almost negligible. The total potential is attractive in the whole range. In the 3D_1 channel, only the σ -exchange provides considerably attractive force. As a result, the total potential is repulsive in the short-range, less than 0.4 fm, while weakly attractive in the range $0.4 < r < 1.5$ fm. In the ${}^3S_1 \leftrightarrow {}^3D_1$ transition potential, the contributions of the ρ - and π -exchanges cancel each other significantly. As a result, the total potential is weakly attractive. Although the exchanged bosons for the $(R, I) = (\bar{3}, 1/2)$ case are different from those for the $(R, I) = (\bar{3}, 0)$ case, the total potentials for both of the two cases are very similar, see Fig. 1.

The numerical results for systems $(R, I) = (\bar{3}, 0)$ and $(\bar{3}, 1/2)$ are given in Table IV. Although the results depend on the cutoff, one can see clearly that for both of the two systems belonging to the $\bar{3}$ -representation, there exist loosely bound states with binding energies around a few MeV for a reasonable cutoff around 1.2 GeV. To investigate the effect of the short-range interaction in forming the bound states, we also present the results without the contact delta interaction. We find that the binding energy almost doubles for the same cutoff once the delta interaction is switched off since the contact interaction is repulsive. But the qualitative features do not change very much. We also notice that the probability of the D wave is tiny, less than 0.4%. This is not surprising since the potential for the transition ${}^3S_1 \leftrightarrow {}^3D_1$ is very weak. The radial wave function $u(r) = y(r)r$ for the individual channel is shown in Fig. 2. We conclude that the systems of the $\bar{3}$ -representation are good candidates of the deuteron-like states.

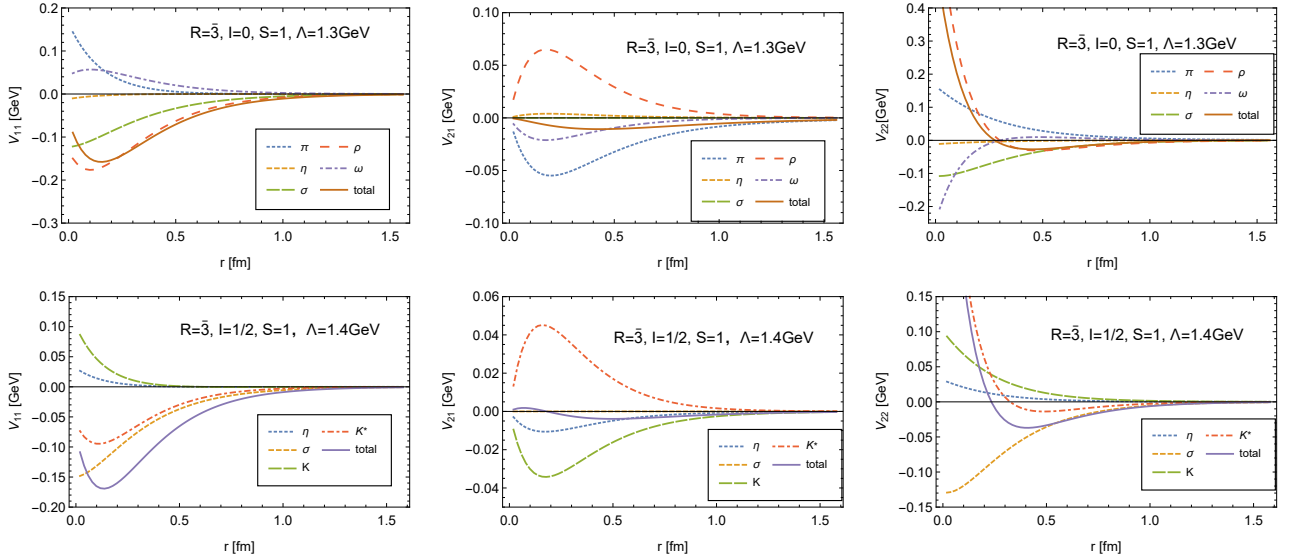


FIG. 1: The interaction potentials for the systems of the $\bar{3}$ -representation ($S = 1$). V_{11} , V_{12} and V_{22} denote the ${}^3S_1 \leftrightarrow {}^3S_1$, ${}^3S_1 \leftrightarrow {}^3D_1$ and ${}^3D_1 \leftrightarrow {}^3D_1$ transitions potentials, respectively. The upper panel is for $(R, I) = (\bar{3}, 0)$ while the lower panel is for $(R, I) = (\bar{3}, 1/2)$.

TABLE IV: The binding solutions for the $B_{cc}B_{cc}$ systems. “ Λ ” is the cutoff parameter. “B.E.” means the binding energy while r_{rms} is the root-mean-square radius. P_S is the probability (%) of the S wave.

Systems	With contact term				Without contact term			
	Λ (GeV)	B.E (Mev)	r_{rms} (fm)	P_S (%)	Λ (GeV)	B.E (Mev)	r_{rms} (fm)	P_S (%)
$(\bar{3}, \frac{1}{2})$	1.2	0.56	3.45	99.98	1.2	2.41	1.85	99.96
	1.5	17.76	0.86	99.99	1.5	34.55	0.66	99.99
	1.9	60.58	0.55	99.94	1.9	116.04	0.42	99.93
$(\bar{3}, 0)$	1.1	0.68	3.23	99.74	1.1	3.28	1.66	99.69
	1.3	12.25	1.01	99.79	1.3	25.07	0.77	99.86
	1.5	33.20	0.70	99.93	1.5	61.46	0.55	99.97

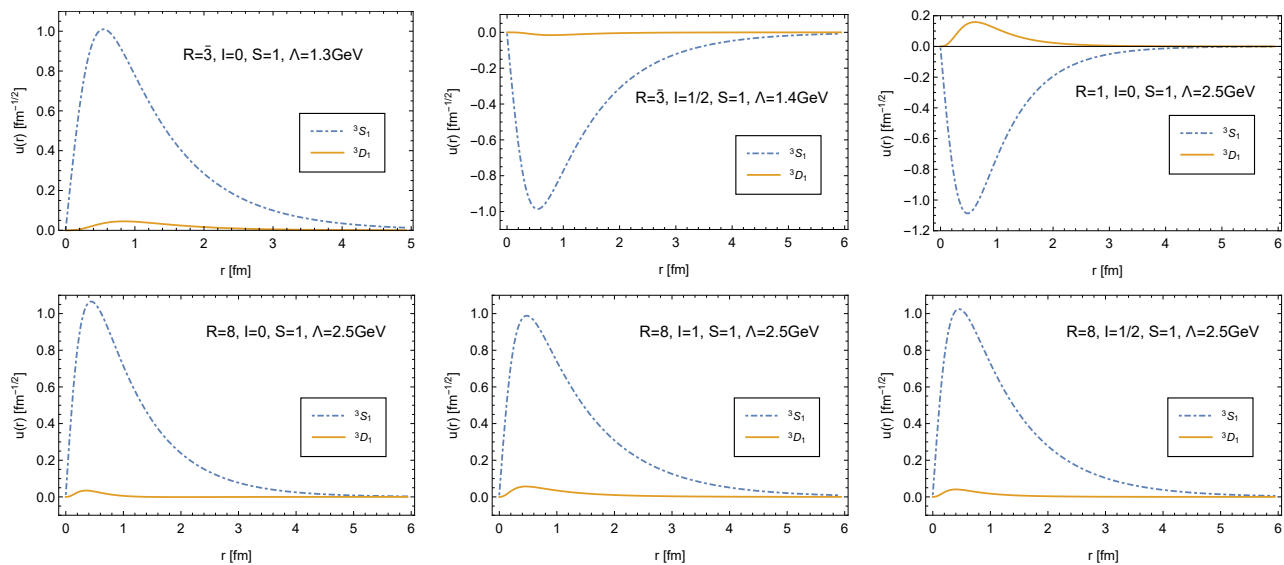


FIG. 2: (Color online). The radial wave functions $u(r) = y(r)r$ for the spin-triplet channels.

2. 6-representation, $S = 0$

The systems of the 6-representation are simpler since they are all spin-singlets. We show the potential for each boson-exchange in Fig. 3. From the plots, one can see clearly that the total potentials for all of the three systems are repulsive in the range, less than 0.4 fm, for the cutoff around 1.5 GeV. The numerical results are given in Table V. For the system $(R, I) = (6, 1)$, we fail to obtain any binding solutions. For the systems $(R, I) = (6, 1/2)$ and $(6, 0)$, we could not obtain binding solutions until we increase the cutoff to be 5.4 GeV and 3.8 GeV respectively. If we switch off the contact delta interaction, a loosely bound state is obtained for $(6, 1)$ with $\Lambda = 1.9$ GeV, for $(6, 1/2)$ with $\Lambda = 1.6$ GeV and for $(6, 0)$ with $\Lambda = 1.5$ GeV. However, the contact delta interaction in the spin-0 systems with 6-representation is strongly repulsive. Moreover, Pauli principle may forbid the four charm quarks at the origin simultaneously. Therefore, we conclude that there do not exist the molecular states for the systems of the 6-representation.

B. $B_{cc}\bar{B}_{cc}$ systems

For the baryon-antibaryon systems, there is no constraint from Pauli Principle. All the systems can be both spin-singlet ($S = 0$) and spin-triplet ($S = 1$). We present the results according to the spin of the system, i.e., spin-singlet

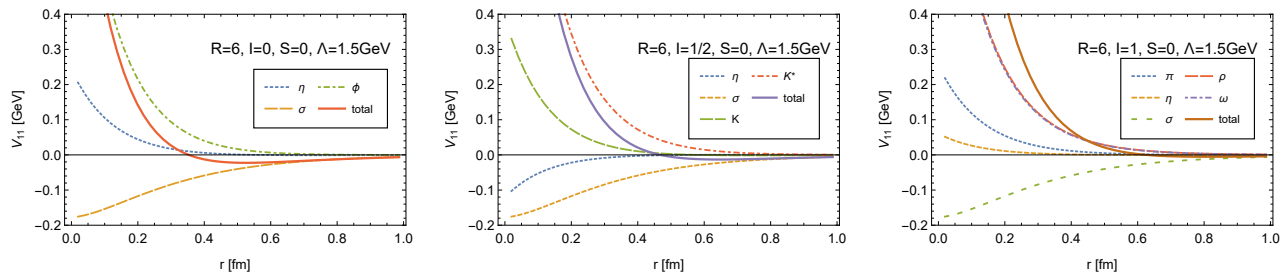


FIG. 3: (Color online). The interaction potentials for the systems of the 6-representation.

TABLE V: The binding solutions for the systems of the 6-representation. “×” means that no binding solutions are obtained.

Systems	With contact term			Without contact term		
	Λ (GeV)	B.E (MeV)	r_{rms} (fm)	Λ (GeV)	B.E (MeV)	r_{rms} (fm)
(6, 1)	×	×	×	1.9	0.31	4.27
				3.0	3.43	1.56
				3.6	5.11	1.31
(6, $\frac{1}{2}$)	5.4	0.14	5.25	1.6	4.69	1.40
	6.6	1.29	2.45	1.9	12.38	0.95
	7.5	2.65	1.80	2.5	31.10	0.65
(6, 0)	3.8	0.10	5.55	1.5	5.50	1.31
	4.5	1.27	2.48	1.7	14.80	0.89
	5.0	2.74	1.80	2.0	34.16	0.64

and spin-triplet. The $S = 0$ and $S = 1$ potentials are shown in Fig. 4 and 5, respectively.

1. $B_{cc}\bar{B}_{cc}$, spin-singlet

For the system $(R, I) = (8, 1/2)$, only η - and σ -exchanges are allowed while all the η -, σ -, π -, ρ - and ω - exchanges contribute to the system $(8, 1)$. For the system $(8, 0)$ and $(1, 0)$, additional K -, K^* - and ϕ -exchanges are also allowed. We give the numerical binding-solution results in Table VI. Interestingly, we obtain a loosely bound state for the system $(R, I) = (8, 1/2)$ for the cutoff in the range $1.5 < \Lambda < 2.0$ GeV, both with and without the contact interaction. For this bound state, both the η - and σ -exchanges supply attractive force, see Fig. 4. From Fig. 6, one can also see that the binding solutions depend weakly on the cutoff parameter, which indicates the system $(R, I) = (8, 1/2)$ is a good candidate of the molecular state.

There also exist loosely bound states for the systems $(R, I) = (8, 1)$ and $(8, 0)$, both with and without the contact interaction for the cutoff in the range $1.5 - 2.0$ GeV. The binding energies are a few MeV and the root-mean-square radii are both around 1 fm. For the system $(8, 1)$, the contributions of the ρ - and ω -exchanges cancel each other significantly. Both of the σ - and π -exchanges provide attractive force while the η -exchange supply the repulsive force. For the system $(8, 0)$, the potential from the K^* -exchange is strongly repulsive. The η - and π -exchanges also provide repulsive force while the potentials from the ρ -, ω -, σ -, ϕ - and K - exchanges are attractive, see Fig. 4. These two interesting states are also good candidates of the molecular states.

Although we obtain binding solutions for the system $(1, 0)$, the results depend strongly on the cutoff parameter. After removing the contact interaction, a loosely bound state is obtained for the cutoff around $1.1 < \Lambda < 1.6$ GeV. This system might be a molecule candidate.

From Table VI, one can see that the binding is larger when the contact interaction is included. The contact

TABLE VI: The binding solutions of the spin-singlet $B_{cc}\bar{B}_{cc}$ systems.

Systems	With contact term			Without contact term		
	Λ (GeV)	B.E. (MeV)	r_{rms} (fm)	Λ (GeV)	B.E. (MeV)	r_{rms} (fm)
(8, 1)	1.3	0.11	5.41	1.5	0.26	4.49
	1.6	3.75	1.50	1.6	0.83	2.87
	2.0	13.49	0.89	1.9	3.77	1.50
	2.5	30.25	0.64	2.6	13.28	0.89
(8, $\frac{1}{2}$)	1.4	0.18	4.93	1.5	0.05	5.96
	1.6	2.00	1.96	1.8	1.70	2.11
	2.0	9.54	1.02	2.0	3.53	1.54
	2.5	23.55	0.70	2.5	9.10	1.04
(8, 0)	1.4	0.42	3.84	1.4	0.04	6.06
	1.6	2.34	1.85	1.6	1.08	2.59
	2.0	9.25	1.04	2.0	4.96	1.35
	2.5	21.36	0.74	2.5	10.63	0.98
(1, 0)	1.05	1.71	2.17	1.1	0.08	5.71
	1.1	11.68	0.99	1.2	1.00	2.74
	1.2	74.73	0.48	1.3	2.58	1.83
	1.3	216.46	0.32	1.6	9.40	1.09

interactions of the π , ρ and σ exchanges (the isospin factor is set to 1) for the spin-singlet system are shown in Fig. 7. One can see clearly that the contribution of the π and ρ exchanges to the contact interaction are roughly equal, and both are repulsive. The σ exchange contribution is negligible. From Table III, the summation of the isospin factors of the vector mesons for 8-representation systems are 0. Thus, the vector meson exchange contribution to the contact interaction almost cancels out. The attractive contact interaction mainly arise from the pseudoscalar exchanges. For the 1-representation system, the attractive contact interaction is the result of the cancellation of the vector meson exchanges with the pseudoscalar exchanges.

2. $B_{cc}\bar{B}_{cc}$, spin-triplet

For the spin-triplet case, we show the potentials in Fig. 5 and present the binding solutions in Table VII. Similar to the spin-singlet case, we also obtain loosely bound states for a reasonable cutoff in the spin-triplet sector. These states are very interesting and are good candidates of the molecular states. For example, we obtain a loosely bound state for the system $(R, I) = (8, 1)$ which has binding energy 0.05 – 3.47 MeV and root-mean-square radius 5.98 – 1.56 fm for the cutoff around 1.5 – 2.0 GeV. With the same cutoff, a loosely bound state of the system $(8, 1/2)$ with binding energy 0.27 – 4.65 MeV and root-mean-square radius 4.45 – 1.39 fm is obtained. Similarly, for the system $(8, 0)$, we obtain a loosely bound state with binding energy 0.06 – 7.01 MeV for the cutoff around 1.3 – 2.0 GeV. All these three states $(R, I) = (8, 1)$, $(8, 1/2)$, and $(8, 0)$ are good candidates of the molecular states. We also obtain binding solutions for the system of the 1-representation $(1, 0)$. Unfortunately, the results depend strongly on the cutoff.

Very interestingly, we also find that for the spin-triplet case the results change very little by removing the contact interaction. This means that the contact interaction plays a minor role in the formation of the bound states in the spin-triplet sector. The contribution of the D -wave for the systems belonging to the 8-representation is less than 0.4%, similar to that in the baryon-baryon case. In contrast, the D -wave plays a more important role in the 1-representation

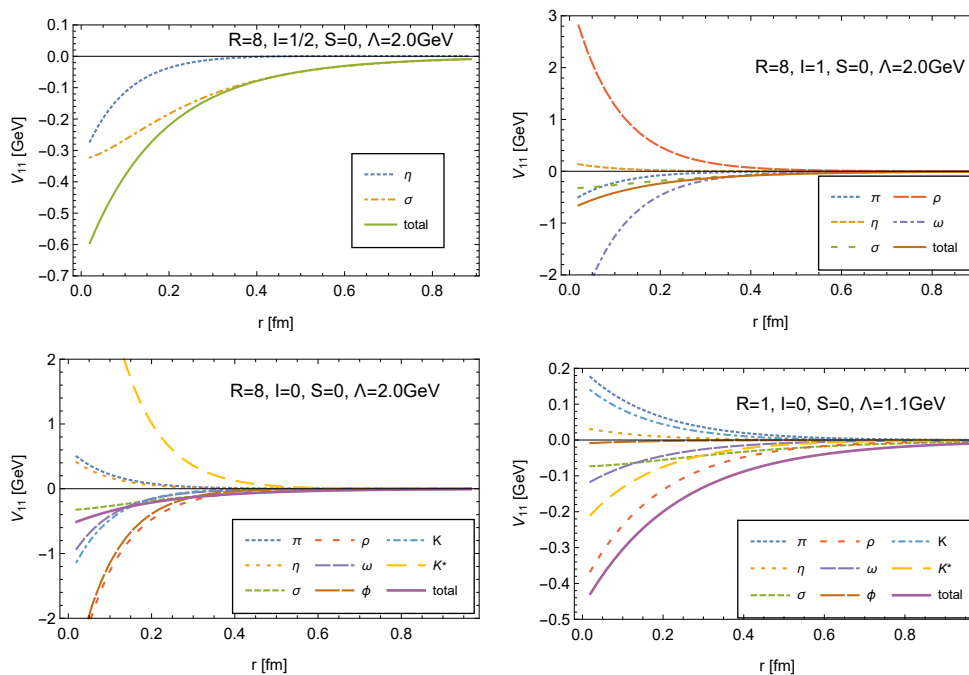


FIG. 4: (Color online). The interaction potentials of the spin-singlet $B_{cc}\bar{B}_{cc}$ systems.

system for $\Lambda = 1.1$ GeV.

Compared with the spin-triplet systems, the spin-singlet systems have a weaker dependence on the contact interaction. For the S wave, the contact interaction only arise from the spin-spin interaction. And the matrix elements of the spin-spin operator for $S = 1$ is 1 while that for $S = 0$ is -3 . Thus the results for the spin-triplet systems change less by removing the contact interaction, compared with the spin-singlet systems.

IV. DISCUSSIONS AND CONCLUSIONS

In this work, we have performed a systematic investigation of the possible deuteron-like states composed of a pair of doubly charmed spin- $\frac{1}{2}$ baryons or one doubly charmed baryon and one doubly charmed antibaryon. In the spin-triplet sector we take into account mixing between the 3S_1 and 3D_1 channels. The present formalism can also be extended to the loosely bound systems composed of one spin- $\frac{1}{2}$ and one spin- $\frac{3}{2}$ or two spin- $\frac{3}{2}$ baryons.

For the spin-triplet $B_{cc}B_{cc}$ systems, we obtain two loosely bound states for $(R, I) = (\bar{3}, 1/2)$ and $(\bar{3}, 0)$. Their binding energies are from a few MeV to tens of MeV and root-mean-square radii from 1 fm to a few fm for the cutoff around 1.2 – 1.5 GeV. They are good candidates of the molecular states. In the spin-singlet sector, the potentials are not strong enough to form bound states for $(R, I) = (6, 1)$, $(6, 1/2)$ and $(6, 0)$ with a reasonable cutoff value.

For the $B_{cc}\bar{B}_{cc}$ systems, the spin-singlet and spin-triplet cases are similar. Very interestingly, we obtain loosely bound states for the spin-singlet and spin-triplet systems with $(R, I) = (8, 1)$, $(8, 1/2)$ and $(8, 0)$. They have binding energies around a few MeV and root-mean-square radii around a few fm. They are also very good candidates of the molecular states in the framework of the one-boson-exchange-potential model. We also notice that the contact interaction plays a minor role in the formation of the bound states for the $B_{cc}\bar{B}_{cc}$ systems. The D-wave probability is tiny for most of the spin-triplet channels.

Theoretical explorations of the exotic states containing multiple heavy quarks first appeared nearly three decades ago [66]. Recently these charming states are gaining more and more interest. In the past several years, many events with four heavy quarks ($QQ\bar{Q}\bar{Q}$) have been reported experimentally [40–44]. There are heated theoretical discussions of the exotic resonances containing four heavy quarks recently [45–50]. The $B_{cc}\bar{B}_{cc}$ molecular states may be produced at LHC in the near future. Once produced, they may decay into very characteristic final states containing one or two charmonia, including (1) two charmonia plus one or more light mesons/photons; (2) one charmonium and a $D^{(*)}\bar{D}^{(*)}$ pair; (3) one charmonium plus some photons or light mesons etc. They may also decay into many light mesons or several hard photons. The $B_{cc}\bar{B}_{cc}$ molecular states lie close to the mass threshold of two doubly charmed baryons, which provides a clue to identify them unambiguously. For example, these molecular states may appear around $7 \sim 7.5$

TABLE VII: The binding solutions of the spin-triplet $B_{cc}\bar{B}_{cc}$ systems.

Systems	With contact term				Without contact term			
	Λ (GeV)	B.E. (MeV)	r_{rms} (fm)	P_S (%)	Λ (GeV)	B.E. (MeV)	r_{rms} (fm)	P_S (%)
(8, 1)	1.5	0.05	5.98	99.97	1.5	0.25	4.56	99.95
	1.6	0.40	3.91	99.94	1.6	0.80	2.95	99.92
	2.0	3.47	1.56	99.85	1.9	3.65	1.53	99.86
	2.5	8.95	1.06	99.76	2.3	8.96	1.05	99.79
(8, $\frac{1}{2}$)	1.5	0.27	4.45	99.99	1.5	0.47	3.67	99.99
	1.6	0.81	2.92	99.99	1.6	1.19	2.48	99.99
	2.0	4.65	1.39	99.96	1.9	4.55	1.40	99.96
	2.5	10.85	0.98	99.90	2.3	10.46	0.99	99.92
(8, 0)	1.3	0.06	5.84	99.99	1.3	0.12	5.39	99.99
	1.6	2.13	1.94	99.99	1.6	2.51	1.81	99.99
	2.0	7.01	1.18	99.99	2.0	8.19	1.11	99.99
	2.5	14.00	0.90	99.95	2.5	16.62	0.83	99.95
(1, 0)	1.0	2.32	1.90	99.11	1.0	0.73	3.09	99.35
	1.1	20.33	0.84	98.15	1.1	16.02	0.92	98.09
	1.2	56.70	0.60	97.31	1.2	52.46	0.61	97.23
	1.3	109.41	0.48	96.49	1.3	108.67	0.48	96.47

GeV depending on the mass of Ξ_{bc} . Similarly, we also expect $B_{bc}\bar{B}_{bc}$ and $B_{bb}\bar{B}_{bb}$ types of molecular states. They may lie roughly around 14 GeV and 20 GeV respectively, if we take the mass values of $\Xi_{bc,bb}$ in Ref. [57, 59–61].

Although very difficult to generate experimentally, the bound states of $\Xi_{cc}\Xi_{cc}$ might be stable once produced because Ξ_{cc} decays via weak interaction most likely. There might exist a strong decay mode: $\Xi_{cc}\Xi_{cc} \rightarrow \Omega_{ccc}^{++}A_c$, where A_c is a charmed baryon and Ω_{ccc}^{++} is the triply charmed baryon. The mass estimation of triply charmed baryon can be found in Ref. [55, 67]. Whether the above decay mode exists or not depends on the masses of the Ξ_{cc} and Ω_{ccc}^{++} .

ACKNOWLEDGMENTS

L. Meng is very grateful to G.J. Wang, H.S Li and B. Zhou for very helpful discussions. The authors thank Ulf-G. Meißner and J.-M. Richard for helpful comments. This project is supported by the National Natural Science Foundation of China under Grants NO. 11621131001, 11575008 and 973 program. This work is also supported in part by the DFG and the NSFC through funds provided to the Sino-German CRC 110 ‘‘Symmetries and the Emergence of Structure in QCD’’.

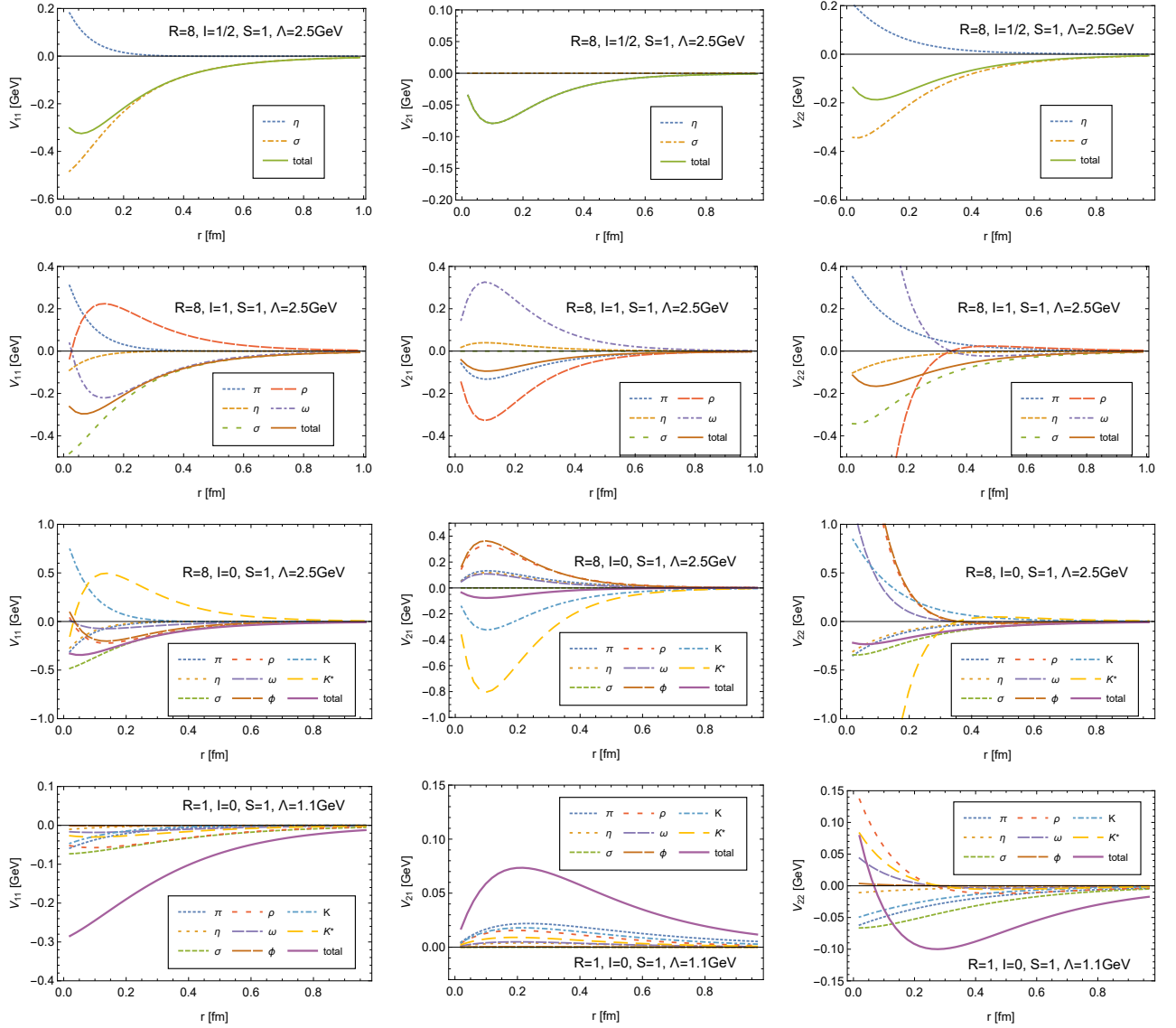


FIG. 5: (Color online). The interaction potentials of the spin-triplet $B_{cc}\bar{B}_{cc}$ systems.

Appendix A: Definitions of some functions and Fourier transform formulae

The definitions of the functions H_i are [30],

$$\begin{aligned}
 H_0(\Lambda, m, r) &= Y(ur) - \frac{\lambda}{u}Y(\lambda r) - \frac{r\beta^2}{2u}Y(\lambda r), & H_1(\Lambda, m, r) &= Y(ur) - \frac{\lambda}{u}Y(\lambda r) - \frac{r\lambda^2\beta^2}{2u^3}Y(\lambda r), \\
 H_2(\Lambda, m, r) &= Z_1(ur) - \frac{\lambda^3}{u^3}Z_1(\lambda r) - \frac{\lambda\beta^2}{2u^3}Y(\lambda r), & H_3(\Lambda, m, r) &= Z(ur) - \frac{\lambda^3}{u^3}Z(\lambda r) - \frac{\lambda\beta^2}{2u^3}Z_2(\lambda r),
 \end{aligned} \tag{A1}$$

where,

$$\beta^2 = \Lambda^2 - m^2, \quad u^2 = m^2 - Q_0^2, \quad \lambda^2 = \Lambda^2 - Q_0^2,$$

and

$$Y(x) = \frac{e^{-x}}{x}, \quad Z(x) = \left(1 + \frac{3}{x} + \frac{3}{x^2}\right)Y(x), \quad Z_1(x) = \left(\frac{1}{x} + \frac{1}{x^2}\right)Y(x), \quad Z_2(x) = (1+x)Y(x).$$

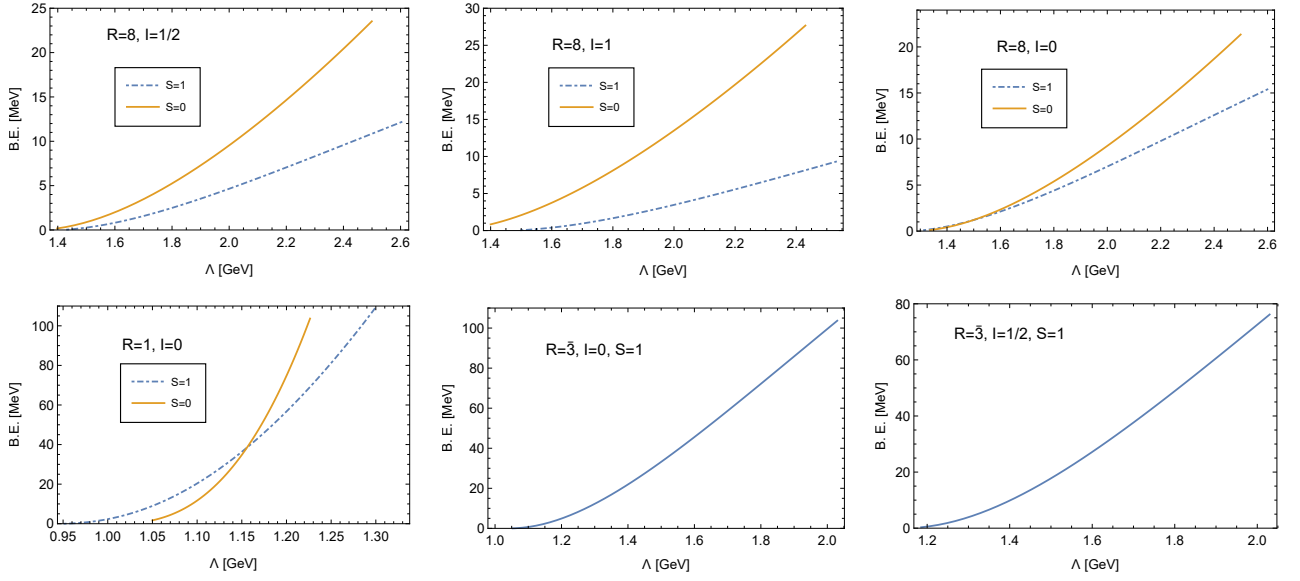


FIG. 6: (Color online). The binding energy versus the cutoff parameter. The contact interaction is included.

In our case all heavy hadrons have the same masses, we have

$$Q_0^2 = \left(\sqrt{m_f^2 + \mathbf{p}_f^2} - \sqrt{m_i^2 + \mathbf{p}_i^2} \right)^2 \approx \frac{(\mathbf{p}_i + \mathbf{p}_f)^2 Q^2}{4m_{\Xi_{cc}}^2}. \quad (\text{A2})$$

Thus Q_0^2 is a high-order term and can be directly dropped out.

Without the form factor, one makes Fourier transformation and obtains

$$\frac{1}{u^2 + Q^2} \rightarrow \frac{e^{-ur}}{4\pi r} = \frac{u}{4\pi} Y(ur), \quad (\text{A3})$$

$$\frac{Q}{u^2 + Q^2} \rightarrow -i\nabla \left(\frac{u}{4\pi} Y(ur) \right) = i \frac{u^3}{4\pi} Z_1(ur) \mathbf{r}, \quad (\text{A4})$$

$$\frac{Q^2}{u^2 + Q^2} \rightarrow -\frac{u^3}{4\pi} Y(ur) + \delta^{(3)}(\mathbf{r}), \quad (\text{A5})$$

$$\frac{Q_i Q_j}{u^2 + Q^2} \rightarrow -\frac{u^3}{12\pi} [Z(ur) k_{ij} + Y(ur) \delta_{ij}] + \frac{1}{3} \delta^{(3)}(\mathbf{r}) \delta_{ij}, \quad (\text{A6})$$

where $k_{ij} = 3 \frac{r_i r_j}{r^2} - \delta_{ij}$. Clearly, there exist terms with a delta function $\delta^{(3)}(\mathbf{r})$ in Eqs. (A5-A6). In the current work, we call these terms the contact interaction or delta interaction. The very short-range interactions accounted by the heavier-meson exchange are not taken into account in the current analysis. In Ref.[68], the short-range annihilation force is introduced by fitting the data for the nucleon-antinucleon system. However, introducing such short-range interaction is not feasible for the $\Xi_{cc}\bar{\Xi}_{cc}$ systems due to the lack of the experimental data. Luckily, the $\Xi_{cc}\bar{\Xi}_{cc}$ annihilation force is of extremely short range around 0.02 fm. We are mainly interested in the loosely bound molecular states which should not depend sensitively on the short-range dynamics.

After introducing the form factor, the Fourier transformation formulae read

$$\begin{aligned} \frac{1}{u^2 + Q^2} \mathcal{F}^2(Q) &\rightarrow \frac{u}{4\pi} H_0(\Lambda, m, r), \\ \frac{Q^2}{u^2 + Q^2} \mathcal{F}^2(Q) &\rightarrow -\frac{u^3}{4\pi} H_1(\Lambda, m, r), \\ \frac{Q}{u^2 + Q^2} \mathcal{F}^2(Q) &\rightarrow \frac{i u^3}{4\pi} \mathbf{r} H_2(\Lambda, m, r), \\ \frac{Q_i Q_j}{u^2 + Q^2} \mathcal{F}^2(Q) &\rightarrow -\frac{u^3}{12\pi} [H_3(\Lambda, m, r) k_{ij} + H_1(\Lambda, m, r) \delta_{ij}]. \end{aligned} \quad (\text{A7})$$

One can also get the results without the contact interaction term by a simple replacement in the above equations,

$$H_1(\Lambda, m, r) \rightarrow H_0(\Lambda, m, r). \quad (\text{A8})$$

We show the interaction potentials both with and without the contact interaction in Figs. (7-8). We take the π , ρ and σ exchange forces an example. The isospin factors are set to 1. From the plots, one can see clearly that the contact interaction plays a minor role for the σ exchange while its contribution is important in the range $r < 0.4$ fm for the π and ρ exchanges.

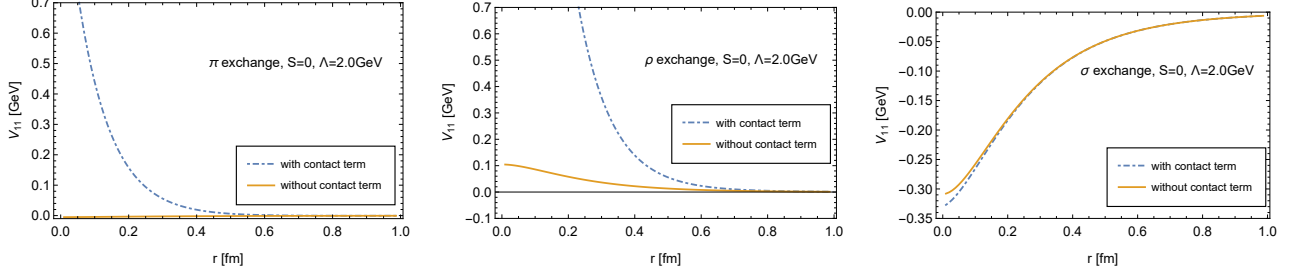


FIG. 7: (Color online). The potentials with/without the contact terms for the 1S_0 channels. The isospin factors are set to 1.

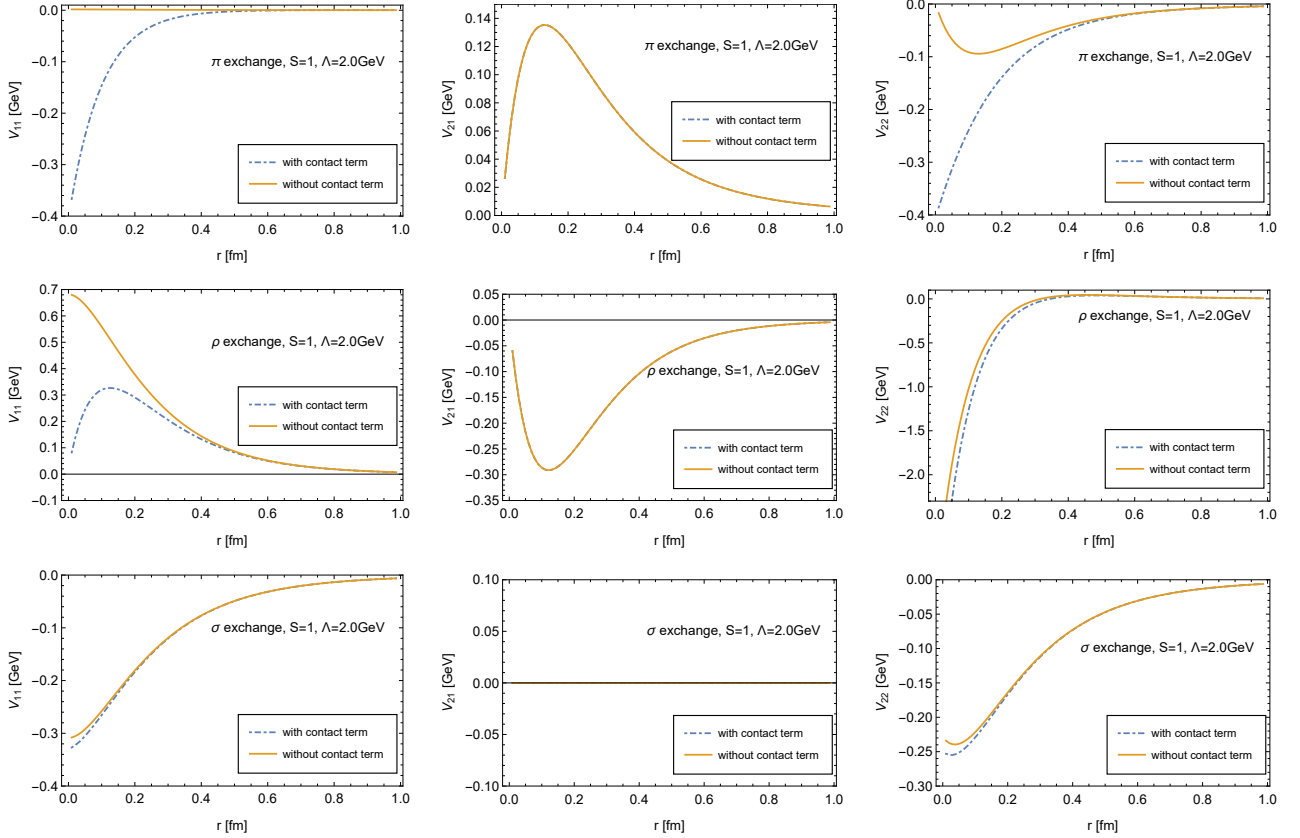


FIG. 8: (Color online). The potentials with/without the contact terms for the coupled $^3S_1 - ^3D_1$ channels. The isospin factors are set to 1.

Appendix B: Matrix elements of the operators

In the present work, we encounter the following operators,

- Spin-spin operator:

$$\boldsymbol{\sigma}_1 \cdot \boldsymbol{\sigma}_2, \quad (\text{B1})$$

- Spin-orbit operator:

$$\mathbf{L} \cdot \mathbf{S}, \quad \mathbf{L} \cdot \mathbf{S}_1, \quad \mathbf{L} \cdot \mathbf{S}_2, \quad (\text{B2})$$

- Tensor operator:

$$S_{12}(\hat{r}) = 3(\boldsymbol{\sigma}_1 \cdot \hat{r})(\boldsymbol{\sigma}_2 \cdot \hat{r}) - \boldsymbol{\sigma}_1 \cdot \boldsymbol{\sigma}_2. \quad (\text{B3})$$

For the spin-spin operator, one has

$$\begin{aligned} \boldsymbol{\sigma}_1 \cdot \boldsymbol{\sigma}_2 &= 2(\mathbf{S}^2 - \mathbf{S}_1^2 - \mathbf{S}_2^2) \\ &= 2\left[S(S+1) - \frac{3}{2}\right]. \end{aligned} \quad (\text{B4})$$

The results are independent with the orbit angular momentum. For spin-singlet and spin-triplet, the matrix elements of the spin-spin interaction are -3 and 1 respectively.

For the spin-orbit operator one has,

$$\mathbf{L} \cdot \mathbf{S} = \frac{1}{2}(\mathbf{J}^2 - \mathbf{L}^2 - \mathbf{S}^2) \quad (\text{B5})$$

$$= \frac{1}{2}[J_i(J_i+1) - L_i(L_i+1) - S_i(S_i+1)] \quad (\text{B6})$$

The results for 1S_0 , 3S_1 and 3D_1 systems are 0, 0 and -3/2 respectively. As for the $\mathbf{L} \cdot \mathbf{S}_{A(B)}$ type interaction, the spin-orbit interaction vanishes for 1S_0 , 3S_1 systems. For the 3D_1 system, the spin wave function is symmetric. The matrix elements of $\mathbf{L} \cdot \mathbf{S}_A$ and $\mathbf{L} \cdot \mathbf{S}_B$ are the same, which are the half of the matrix element of the operator $\mathbf{L} \cdot \mathbf{S}$.

The tensor operator is the scalar product of two rank-2 operator $Y_{2,m}(\hat{r})$ and $T_{2,m}$,

$$S_{12} = \sum_{m=-2}^2 4\sqrt{\frac{6\pi}{5}} T_{2,m} Y_{2,m}^*(\hat{r}), \quad (\text{B7})$$

where $Y_{2,m}(\hat{r})$ is the spherical harmonic function of degree 2, and $T_{2,m}$ is rank-2 tensor operator constructed from the total spin operator \mathbf{S} ,

$$\begin{aligned} T_{2,\pm 2} &= \frac{3}{8\pi} (S_x \pm iS_y)^2, \\ T_{2,\pm 1} &= \mp \frac{3}{8\pi} [S_z (S_x \pm iS_y) + (S_x \pm iS_y) S_z], \\ T_{2,0} &= \sqrt{\frac{1}{6}} \frac{3}{4\pi} (3S_z^2 - \mathbf{S}^2). \end{aligned} \quad (\text{B8})$$

One can obtain the matrix elements of the tensor operator using the Wigner-Echart theorem.

-
- [1] S. K. Choi *et al.* [Belle Collaboration], Phys. Rev. Lett. **91**, 262001 (2003)
- [2] B. Aubert *et al.* [BaBar Collaboration], Phys. Rev. Lett. **95**, 142001 (2005)
- [3] M. Ablikim *et al.* [BESIII Collaboration], Phys. Rev. Lett. **110**, 252001 (2013)
- [4] Z. Q. Liu *et al.* [Belle Collaboration], Phys. Rev. Lett. **110**, 252002 (2013)
- [5] T. Aaltonen *et al.* [CDF Collaboration], Phys. Rev. Lett. **102**, 242002 (2009)
- [6] K.-F. Chen *et al.* [Belle Collaboration], Phys. Rev. D **82**, 091106 (2010)
- [7] R. Aaij *et al.* [LHCb Collaboration], Phys. Rev. Lett. **115**, 072001 (2015)
- [8] H. X. Chen, W. Chen, X. Liu and S. L. Zhu, Phys. Rept. **639**, 1 (2016)
- [9] M. B. Voloshin and L. B. Okun, JETP Lett. **23**, 333 (1976) [Pisma Zh. Eksp. Teor. Fiz. **23**, 369 (1976)].
- [10] A. De Rujula, H. Georgi and S. L. Glashow, Phys. Rev. Lett. **38**, 317 (1977).
- [11] N. A. Tornqvist, Z. Phys. C **61**, 525 (1994)
- [12] N. A. Tornqvist, Phys. Rev. Lett. **67**, 556 (1991).
- [13] M. Mai and U. G. Meißner, Nucl. Phys. A **900** (2013) 51.
- [14] J. M. M. Hall, W. Kamleh, D. B. Leinweber, B. J. Menadue, B. J. Owen, A. W. Thomas and R. D. Young, Phys. Rev. Lett. **114**, 132002 (2015).
- [15] U. Straub, Z. Y. Zhang, K. Braeuer, A. Faessler, S. B. Khadkikar and G. Luebeck, Nucl. Phys. A **508**, 385C (1990).
- [16] F. Huang and Z. Y. Zhang, Phys. Rev. C **70**, 064004 (2004)
- [17] L. R. Dai, Z. Y. Zhang and Y. W. Yu, Chin. Phys. Lett. **23**, 3215 (2006).
- [18] D. Zhang, F. Huang, L. R. Dai, Y. W. Yu and Z. Y. Zhang, Phys. Rev. C **75**, 024001 (2007)
- [19] L. Chen, H. Pang, H. Huang, J. Ping and F. Wang, Phys. Rev. C **76**, 014001 (2007)
- [20] J. L. Ping, H. X. Huang, H. R. Pang, F. Wang and C. W. Wong, Phys. Rev. C **79**, 024001 (2009)
- [21] H. Huang, P. Xu, J. Ping and F. Wang, Phys. Rev. C **84**, 064001 (2011)
- [22] M. Chen, H. Huang, J. Ping and F. Wang, Phys. Rev. C **83**, 015202 (2011).
- [23] X. Liu, Z. G. Luo, Y. R. Liu and S. L. Zhu, Eur. Phys. J. C **61**, 411 (2009)
- [24] X. Liu and S. L. Zhu, Phys. Rev. D **80**, 017502 (2009) Erratum: [Phys. Rev. D **85**, 019902 (2012)]
- [25] Y. R. Liu, X. Liu, W. Z. Deng and S. L. Zhu, Eur. Phys. J. C **56**, 63 (2008)
- [26] X. Liu, Y. R. Liu, W. Z. Deng and S. L. Zhu, Phys. Rev. D **77**, 034003 (2008)
- [27] X. Liu, Y. R. Liu, W. Z. Deng and S. L. Zhu, Phys. Rev. D **77**, 094015 (2008)
- [28] L. Zhao, L. Ma and S. L. Zhu, Nucl. Phys. A **942**, 18 (2015)
- [29] L. Zhao, L. Ma and S. L. Zhu, Phys. Rev. D **89**, 094026 (2014)
- [30] N. Li and S. L. Zhu, Phys. Rev. D **86**, 014020 (2012)
- [31] N. Lee, Z. G. Luo, X. L. Chen and S. L. Zhu, Phys. Rev. D **84**, 014031 (2011)
- [32] J. Vijande, A. Valcarce, J. M. Richard and P. Sorba, Phys. Rev. D **94**, 034038 (2016)
- [33] T. F. Caramés and A. Valcarce, Phys. Rev. D **92**, 034015 (2015)
- [34] H. Huang, J. Ping and F. Wang, Phys. Rev. C **89**, 035201 (2014)
- [35] S. M. Gerasyuta and E. E. Matskevich, Int. J. Mod. Phys. E **21**, 1250058 (2012)
- [36] Y. R. Liu and M. Oka, Phys. Rev. D **85**, 014015 (2012)
- [37] W. Meguro, Y. R. Liu and M. Oka, Phys. Lett. B **704**, 547 (2011)
- [38] F. Frömel, B. Juliá-Díaz, D.O. Riska, Nucl. Phys. A **750**, 337 (2005)
- [39] B. Juliá-Díaz, D.O. Riska, Nucl. Phys. A **755**, 431 (2005)
- [40] R. Aaij *et al.* [LHCb Collaboration], Phys. Lett. B **707**, 52 (2012)
- [41] V. Khachatryan *et al.* [CMS Collaboration], JHEP **1409**, 094 (2014)
- [42] V. M. Abazov *et al.* [D0 Collaboration], Phys. Rev. Lett. **116**, 082002 (2016)
- [43] Kamuran Dilsiz, on behalf of CMS Collaboration, presented at APS April Meeting 2016, see <https://absuploads.aps.org/presentation.cfm?pid=11931>.
- [44] Maksat Haytmyradov, on behalf of CMS Collaboration, presented at APS April Meeting 2016, see <https://absuploads.aps.org/presentation.cfm?pid=12160>.
- [45] Y. Bai, S. Lu and J. Osborne, arXiv:1612.00012 [hep-ph].
- [46] M. Karliner, S. Nussinov and J. L. Rosner, Phys. Rev. D **95**, 034011 (2017)
- [47] Z. G. Wang, arXiv:1701.04285 [hep-ph].
- [48] W. Chen, H. X. Chen, X. Liu, T. G. Steele and S. L. Zhu, arXiv:1605.01647 [hep-ph].
- [49] J. Wu, Y. R. Liu, K. Chen, X. Liu and S. L. Zhu, arXiv:1605.01134 [hep-ph].
- [50] N. Brambilla, G. Krein, J. Tarrs Castell and A. Vairo, Phys. Rev. D **93**, 054002 (2016)
- [51] H. Yukawa, Proc. Phys. Math. Soc. Jap. **17**, 48 (1935) [Prog. Theor. Phys. Suppl. **1**, 1].
- [52] M. Mattson *et al.* [SELEX Collaboration], Phys. Rev. Lett. **89**, 112001 (2002)
- [53] A. Ocherashvili *et al.* [SELEX Collaboration], Phys. Lett. B **628**, 18 (2005)
- [54] J. Engelfried [SELEX Collaboration], eConf C **0610161**, 003 (2006), arXiv:hep-ex/0702001v1
- [55] A. P. Martynenko, Phys. Lett. B **663**, 317 (2008)
- [56] Z. Shah and A. K. Rai, Eur. Phys. J. C **77**, 129 (2017)
- [57] M. Karliner and J. L. Rosner, Phys. Rev. D **90**, 094007 (2014)
- [58] T. Yoshida, E. Hiyama, A. Hosaka, M. Oka and K. Sadato, Phys. Rev. D **92**, 114029 (2015)

- [59] Z. F. Sun, Z. W. Liu, X. Liu and S. L. Zhu, Phys. Rev. D **91**, 094030 (2015).
- [60] Z. F. Sun and M. J. Vicente Vacas, Phys. Rev. D **93**, 094002 (2016)
- [61] S. J. Brodsky, F. K. Guo, C. Hanhart and U.-G. Meißner, Phys. Lett. B **698**, 251 (2011).
- [62] R. Machleidt, Phys. Rev. C **63**, 024001 (2001)
- [63] R. Machleidt, K. Holinde and C. Elster, Phys. Rept. **149**, 1 (1987).
- [64] X. Cao, B. S. Zou and H. S. Xu, Phys. Rev. C **81**, 065201 (2010)
- [65] C. Patrignani *et al.* [Particle Data Group], Chin. Phys. C **40**, 100001 (2016).
- [66] K.-T. Chao, Zeit. Phys. C7, 317 (1981); J. -P. Ader, J. -M. Richard, and P. Taxil, Phys. Rev. D25, 2370 (1982).
- [67] Z. S. Brown, W. Detmold, S. Meinel and K. Orginos, Phys. Rev. D **90**, 094507 (2014)
- [68] L. Y. Dai, J. Haidenbauer and U. G. Meißner, arXiv:1702.02065 [nucl-th].